

Table III. Univariate analysis of disease-free survival.

Characteristics	n	Hazard ratio	p-value
Age (years)			0.2987
<65	63	Ref.	
≥65	76	1.239	
Gender			0.3658
Male	113	Ref.	
Female	26	0.785	
HBV infection			0.3692
Present	26	Ref.	
Absent	113	0.798	
HCV infection			0.2871
Present	85	Ref.	
Absent	54	1.244	
Child-Pugh grade			0.5886
A	115	Ref.	
B	24	0.8681	
Cirrhosis			0.3820
Absent	78	Ref.	
Present	61	1.194	
α-fetoprotein (ng/ml)			0.1128
<100	93	Ref.	
≥100	46	1.395	
PIVKA-II (mAU/ml)			0.4261
<40	46	Ref.	
≥40	93	1.193	
Tumor size (cm)			0.5323
<3	65	Ref.	
≥3	74	0.881	
Tumor multiplicity			0.0143
Single	102	Ref.	
Multiple	37	1.736	
Macroscopic portal invasion			0.2075
Absent	124	Ref.	
Present	15	1.477	
Stage (TNM)			0.3271
I/II	127	Ref.	
III A/III B	12	1.410	
Histological grade			0.1678
Well/moderately	82	Ref.	
Poorly	57	1.321	
Microscopic portal vein invasion			0.0042
Absent	88	Ref.	
Present	51	1.801	
Microscopic intrahepatic metastasis			0.0007
Absent	104	Ref.	
Present	35	2.185	

Table III. Continued.

Characteristics	n	Hazard ratio	p-value
<i>EFNA1</i>			0.0113
Low expression	69	Ref.	
High expression	70	1.701	
<i>EPHA2</i>			0.4044
Low expression	69	Ref.	
High expression	70	1.185	

Ref., reference; HBV, hepatitis B virus; HCV, hepatitis C virus; PIVKA-II, proteininduced by vitamin K absence or antagonist II; well/moderately, well or moderately differentiated hepatocellular carcinoma; poorly, poorly differentiated hepatocellular carcinoma.

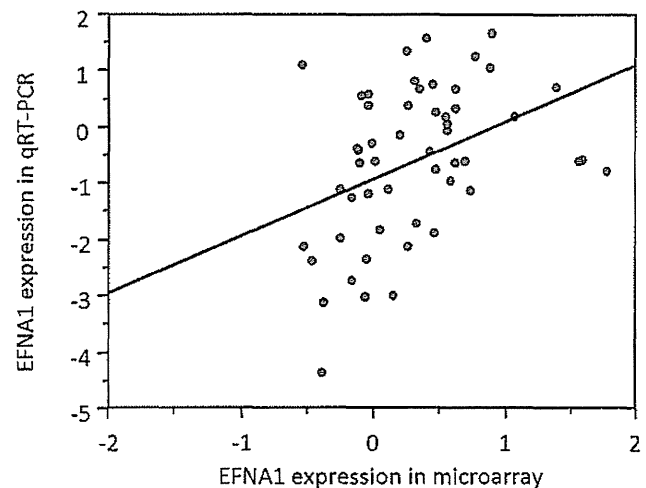


Figure 3. Correlation of *EFNA1* expression according to microarray data and quantitative reverse transcription PCR (qRT-PCR). qRT-PCR data were significantly correlated with the microarray data in all 53 of the hepatocellular carcinoma samples that were tested.

patients with high *EFNA1* expression had significantly shorter disease-free survival (DFS) than those with low *EFNA1* expression based on both microarray (Fig. 4A) and qRT-PCR (Fig. 4B) data. *EPHA2* expression was not correlated with the prognosis for HCC after curative resection (Fig. 4C). Univariate analysis for survival revealed that tumor number, microscopic vascular invasion, microscopic intrahepatic metastasis, and *EFNA1* expression were significantly associated with DFS based on microarray data (Table III). Multivariate Cox regression analysis clarified that only *EFNA1* expression remained an independent prognostic factor (Table IV).

## Discussion

*EFNA1* expression was previously reported to be associated with prognosis in early squamous cell cervical carcinoma (31) and colorectal cancer (32). However, the prognostic impact of *EFNA1* in HCC patients remains unknown. The present study

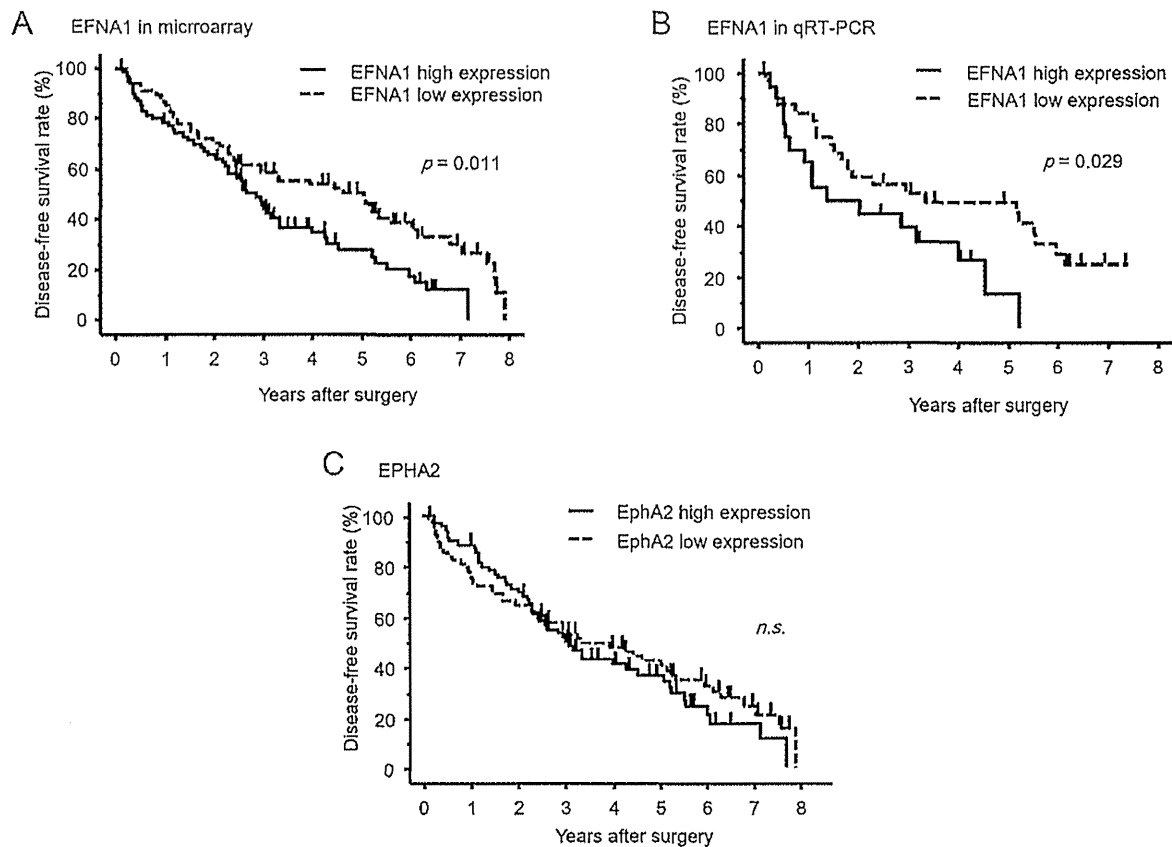


Figure 4. Kaplan-Meier disease-free survival curves for hepatocellular carcinoma patients according to *EFNA1* and *EPHA2* mRNA expression. Patients in the high *EFNA1* mRNA expression group had poorer disease-free survival than those in the low expression group, as shown by both (A) microarray and (C) qRT-PCR analysis. Differences in disease-free survival curves were estimated with the log-rank test for (A) microarray analysis ( $p=0.011$ ) and (B) qRT-PCR analysis ( $p=0.029$ ).

Table IV. Multivariate analysis of disease-free survival.

Characteristics	n	Hazard ratio	95% CI	p-value
Tumor multiplicity				0.8701
Single	102	Ref.		
Multiple	37	1.053	0.565-1.965	
Microscopic portal invasion				0.0574
Absent	88	Ref.		
Present	51	1.505	0.987-2.295	
Microscopic intrahepatic metastasis				0.0611
Absent	104	Ref.		
Present	35	1.848	0.972-3.516	
<i>EFNA1</i> expression				0.0277
Low expression	69	Ref.		
High expression	70	1.605	1.054-2.451	

95% CI, 95% confidence interval; ref., reference.

evaluated the correlation between *EFNA1* mRNA expression levels and prognosis in patients with HCC by microarray analysis of 139 HCC samples and qRT-PCR analysis of 53 samples. The most important finding was that patients with high *EFNA1* expression had a poorer prognosis than

those with low *EFNA1* expression. Furthermore, multivariate analysis demonstrated that *EFNA1* expression was an independent prognostic factor for HCC.

HCC is generally known to occur as a hypervascular tumor, but the rapid proliferation of tumor cells continuously

induces local hypoxia in advanced stages. Angiogenesis is an essential process in carcinogenesis and progression, and several angiogenic factors play important roles in HCC. We previously reported that the expression of vascular endothelial growth factor (VEGF) and angiopoietin-2 is associated with microvascular density in HCC. We also found that high nuclear expression of HIF1A is a significant predictive factor for recurrence after curative resection in HCC patients (9). HIF1A is one of the key transcription factors induced by hypoxic conditions. In the absence of oxygen, it binds to hypoxia-response elements, which activates the expression of numerous hypoxia-response genes, such as VEGF, glucose transporter-1, erythropoietin and *EFNA1* (33).

Two previous studies evaluated the association between expression of *EFNA1* and clinical features in patients with HCC. One report revealed that expression of *EFNA1* and *AFP* was strongly associated and that they induced the expression of genes related to the cell cycle, angiogenesis and cell-cell interactions (34). The other report showed that *EFNA1* mRNA was overexpressed in 90% of HCC cells and *EPHA2* expression was significantly correlated with poor survival in HCC patients (35). Both reports indicated that *EFNA1* and its receptor, *EphA2*, promote proliferation and invasiveness in HCC.

Our result show that *EFNA1* mRNA expression was significantly associated with *EPHA2* mRNA expression, based on microarray data. Moreover, *EFNA1* was a novel independent prognostic factor for HCC. However, *EPHA2* was not a significant prognostic factor. *EPHA2* is a transmembrane receptor tyrosine kinase that is frequently overexpressed in various cancers and is stimulated and phosphorylated by *EFNA1* (36-38). Overexpression of *EPHA2* is associated with aggressive phenotypes and decreased differentiation (37,39). Our results also show *EPHA2* expression tends to correlate with microscopic portal invasion. However, there was no association between *EPHA2* and prognosis in HCC.

In the present study, we used tissue microarrays to analyze not only tumor cells, but also many vascular endothelial cells. *EFNA1* ligand and its receptor, *EPHA2*, were expressed and upregulated in both tumor cells and tumor vessels. In line with the results of the present study, hypoxic conditions are known to upregulate the expression of *EFNA1* in hepatoma cells *in vitro* (34,35). We previously reported that silencing of *EFNA1* in tumor cells inhibits the migration, invasion and proliferation of tumor cells themselves and also inhibits the migration of endothelial cells in coculture experiment (32). Thus, *EFNA1*-mediated interactions between the endothelium and surrounding cells may be critical for vascular sprouting and the penetration of vessels into tumor tissues.

In conclusion, the present findings strongly suggest that *EFNA1* expression is a useful marker for predicting a high risk of recurrence in HCC patients who have undergone curative resection. Anticancer treatments that target *EFNA1* and *EPHA2* may be particularly effective, because they could both suppress tumor neovascularization and directly affect tumor cells. It will be critical to the development of novel anticancer therapies to distinguish the effects of inhibiting *EFNA1/EPHA2* activity on tumor vasculature versus tumor cells.

## References

- Llovet JM, Burroughs A and Bruix J: Hepatocellular carcinoma. *Lancet* 362: 1907-1917, 2003.
- Semenza GL: Hypoxia and cancer. *Cancer Metastasis Rev* 26: 223-224, 2007.
- Noda T, Yamamoto H, Takemasa I, *et al*: PLOD2 induced under hypoxia is a novel prognostic factor for hepatocellular carcinoma after curative resection. *Liver Int* 32: 110-118, 2012.
- Maxwell PH and Ratcliffe PJ: Oxygen sensors and angiogenesis. *Semin Cell Dev Biol* 13: 29-37, 2002.
- Pugh CW and Ratcliffe PJ: Regulation of angiogenesis by hypoxia: role of the HIF system. *Nat Med* 9: 677-684, 2003.
- Semenza GL: Targeting HIF-1 for cancer therapy. *Nat Rev Cancer* 3: 721-732, 2003.
- Zhong H, De Marzo AM, Laughner E, *et al*: Overexpression of hypoxia-inducible factor 1alpha in common human cancers and their metastases. *Cancer Res* 59: 5830-5835, 1999.
- Uemura M, Yamamoto H, Takemasa I, *et al*: Jumonji domain containing 1A is a novel prognostic marker for colorectal cancer: *in vivo* identification from hypoxic tumor cells. *Clin Cancer Res* 16: 4636-4646, 2010.
- Wada H, Nagano H, Yamamoto H, *et al*: Expression pattern of angiogenic factors and prognosis after hepatic resection in hepatocellular carcinoma: importance of angiopoietin-2 and hypoxia-induced factor-1 alpha. *Liver Int* 26: 414-423, 2006.
- Yamada D, Kobayashi S, Yamamoto H, *et al*: Role of the hypoxia-related gene, JMJD1A, in hepatocellular carcinoma: clinical impact on recurrence after hepatic resection. *Ann Surg Oncol* 19 (Suppl 3): S355-S364, 2012.
- Hurwitz H, Fehrenbacher L, Novotny W, *et al*: Bevacizumab plus irinotecan, fluorouracil, and leucovorin for metastatic colorectal cancer. *N Engl J Med* 350: 2335-2342, 2004.
- Cheng AL, Kang YK, Chen Z, *et al*: Efficacy and safety of sorafenib in patients in the Asia-Pacific region with advanced hepatocellular carcinoma: a phase III randomised, double-blind, placebo-controlled trial. *Lancet Oncol* 10: 25-34, 2009.
- Llovet JM, Ricci S, Mazzaferro V, *et al*: Sorafenib in advanced hepatocellular carcinoma. *N Engl J Med* 359: 378-390, 2008.
- Vihanto MM, Plock J, Erni D, Frey BM, Frey FJ and Huynh-Do U: Hypoxia up-regulates expression of Eph receptors and ephrins in mouse skin. *FASEB J* 19: 1689-1691, 2005.
- Yamashita T, Ohneda K, Nagano M, *et al*: Hypoxia-inducible transcription factor-2alpha in endothelial cells regulates tumor neovascularization through activation of ephrin A1. *J Biol Chem* 283: 18926-18936, 2008.
- Bartley TD, Hunt RW, Welcher AA, *et al*: B61 is a ligand for the ECK receptor protein-tyrosine kinase. *Nature* 368: 558-560, 1994.
- Holzman LB, Marks RM and Dixit VM: A novel immediate-early response gene of endothelium is induced by cytokines and encodes a secreted protein. *Mol Cell Biol* 10: 5830-5838, 1990.
- Brantley DM, Cheng N, Thompson EJ, *et al*: Soluble Eph A receptors inhibit tumor angiogenesis and progression *in vivo*. *Oncogene* 21: 7011-7026, 2002.
- Pandey A, Shao H, Marks RM, Polverini PJ and Dixit VM: Role of B61, the ligand for the Eck receptor tyrosine kinase, in TNF-alpha-induced angiogenesis. *Science* 268: 567-569, 1995.
- Cheng N, Brantley DM, Liu H, *et al*: Blockade of EphA receptor tyrosine kinase activation inhibits vascular endothelial cell growth factor-induced angiogenesis. *Mol Cancer Res* 1: 2-11, 2002.
- Deroanne C, Vouret-Craviari V, Wang B and Pouyssegur J: EphrinA1 inactivates integrin-mediated vascular smooth muscle cell spreading via the Rac/PAK pathway. *J Cell Sci* 116: 1367-1376, 2003.
- Ogawa K, Pasqualini R, Lindberg RA, Kain R, Freeman AL and Pasquale EB: The ephrin-A1 ligand and its receptor, EphA2, are expressed during tumor neovascularization. *Oncogene* 19: 6043-6052, 2000.
- Abraham S, Knapp DW, Cheng L, *et al*: Expression of EphA2 and Ephrin A-1 in carcinoma of the urinary bladder. *Clin Cancer Res* 12: 353-360, 2006.
- Brantley-Sieders DM, Fang WB, Hwang Y, Hicks D and Chen J: Ephrin-A1 facilitates mammary tumor metastasis through an angiogenesis-dependent mechanism mediated by EphA receptor and vascular endothelial growth factor in mice. *Cancer Res* 66: 10315-10324, 2006.

25. Liu DP, Wang Y, Koeffler HP and Xie D: Ephrin-A1 is a negative regulator in glioma through downregulation of EphA2 and FAK. *Int J Oncol* 30: 865-871, 2007.
26. Nakamura R, Kataoka H, Sato N, *et al*: EPHA2/EFNA1 expression in human gastric cancer. *Cancer Sci* 96: 42-47, 2005.
27. Nasreen N, Mohammed KA, Lai Y and Antony VB: Receptor EphA2 activation with ephrinA1 suppresses growth of malignant mesothelioma (MM). *Cancer Lett* 258: 215-222, 2007.
28. Noblitt LW, Bangari DS, Shukla S, *et al*: Decreased tumorigenic potential of EphA2-overexpressing breast cancer cells following treatment with adenoviral vectors that express Ephrin-A1. *Cancer Gene Ther* 11: 757-766, 2004.
29. Yamamoto H, Kondo M, Nakamori S, *et al*: JTE-522, a cyclooxygenase-2 inhibitor, is an effective chemopreventive agent against rat experimental liver fibrosis. *Gastroenterology* 125: 556-571, 2003.
30. Yoshioka S, Takemasa I, Nagano H, *et al*: Molecular prediction of early recurrence after resection of hepatocellular carcinoma. *Eur J Cancer* 45: 881-889, 2009.
31. Holm R, de Putte GV, Suo Z, Lie AK and Kristensen GB: Expressions of EphA2 and EphrinA-1 in early squamous cell cervical carcinomas and their relation to prognosis. *Int J Med Sci* 5: 121-126, 2008.
32. Yamamoto H, Tei M, Uemura M, *et al*: Ephrin-A1 mRNA is associated with poor prognosis of colorectal cancer. *Int J Oncol* 42: 549-555, 2013.
33. Harris AL: Hypoxia - a key regulatory factor in tumour growth. *Nat Rev Cancer* 2: 38-47, 2002.
34. Iida H, Honda M, Kawai HF, *et al*: Ephrin-A1 expression contributes to the malignant characteristics of {alpha}-feto-protein producing hepatocellular carcinoma. *Gut* 54: 843-851, 2005.
35. Cui XD, Lee MJ, Yu GR, *et al*: EFNA1 ligand and its receptor EphA2: potential biomarkers for hepatocellular carcinoma. *Int J Cancer* 126: 940-949, 2010.
36. Miyazaki T, Kato H, Fukuchi M, Nakajima M and Kuwano H: EphA2 overexpression correlates with poor prognosis in esophageal squamous cell carcinoma. *Int J Cancer* 103: 657-663, 2003.
37. Zelinski DP, Zantek ND, Stewart JC, Irizarry AR and Kinch MS: EphA2 overexpression causes tumorigenesis of mammary epithelial cells. *Cancer Res* 61: 2301-2306, 2001.
38. Zeng G, Hu Z, Kinch MS, *et al*: High-level expression of EphA2 receptor tyrosine kinase in prostatic intraepithelial neoplasia. *Am J Pathol* 163: 2271-2276, 2003.
39. Walker-Daniels J, Riese DJ, 2nd and Kinch MS: c-Cbl-dependent EphA2 protein degradation is induced by ligand binding. *Mol Cancer Res* 1: 79-87, 2002.

# Mesenchymal phenotype after chemotherapy is associated with chemoresistance and poor clinical outcome in esophageal cancer

JOHJI HARA, HIROSHI MIYATA, MAKOTO YAMASAKI, KEIJIRO SUGIMURA,  
TSUYOSHI TAKAHASHI, YUKINORI KUROKAWA, KIYOKAZU NAKAJIMA,  
SHUJI TAKIGUCHI, MASAKI MORI and YUICHIRO DOKI

Department of Gastroenterological Surgery, Graduate School of Medicine, Osaka University, Osaka 565-0871, Japan

Received March 14, 2012; Accepted May 14, 2012

DOI: 10.3892/or.2013.2876

**Abstract.** The relationship between the epithelial-mesenchymal transition (EMT) and resistance to anticancer treatment has attracted attention in recent years. However, to date, there is no direct clinical evidence for a link between the mesenchymal phenotype and chemoresistance in human malignancies. The expression of EMT-related markers, including E-cadherin, Snail, vimentin, ZEB1,  $\beta$ -catenin and N-cadherin was examined immunohistochemically in 185 tissue samples from patients with esophageal cancer (including 93 patients who received preoperative chemotherapy followed by surgery and 92 patients who underwent surgery without preoperative therapy). The relationship between the expression of the above markers and clinical outcome including prognosis and response to chemotherapy was also examined. The expression of E-cadherin, a marker of epithelial cells, was significantly lower in residual tumors than chemo-naïve tumors ( $P=0.003$ ). The expression of Snail ( $P=0.028$ ), ZEB1 ( $P<0.001$ ) and N-cadherin ( $P=0.001$ ), markers of mesenchymal cells, was higher in residual tumors than in chemo-naïve tumors. The expression of E-cadherin correlated inversely with that of Snail ( $P<0.001$ ). Reduced expression of E-cadherin and increased expression of Snail in residual tumors from patients who received chemotherapy correlated significantly with poor response to chemotherapy and short survival time. Multivariate analysis identified Snail expression as an independent prognostic factor, along with tumor depth, in patients who received preoperative chemotherapy for esophageal cancer. The results suggest transition of residual esophageal cancer cells to mesenchymal phenotype after chemotherapy

and this contributes to resistance to chemotherapy and poor prognosis in patients with esophageal cancer.

## Introduction

Esophageal cancer is one of the most aggressive and lethal malignancies. Surgical treatment is considered the standard management approach for esophageal cancer. However, despite recent advances in surgical technique, the prognosis of patients who undergo surgery alone is poor (1-3). Thus, multimodal treatment such as surgery following neoadjuvant chemotherapy or chemoradiotherapy is advocated. In fact, several clinical trials have shown that such multimodal therapies prolonged survival of patients with esophageal cancer (4-7). However, the reported response rate to chemotherapy in esophageal cancer is only 19-40% (1,2,4,8-10) and chemoresistance has emerged as a serious problem. Thus, there is a need to understand the underlying mechanism of chemoresistance in esophageal cancer.

Epithelial-mesenchymal transition (EMT) is a biologic process that allows a polarized epithelial cell, which normally interacts with the basement membrane via its basal surface, to undergo multiple biochemical changes that enable it to assume a mesenchymal phenotype. The latter phenotype is characterized by enhanced migratory capacity, invasiveness, high resistance to apoptosis and enhanced production of components of the extracellular matrix (ECM) (11). EMT and the reverse process, termed mesenchymal-epithelial transition (MET), play a central role in embryogenesis (type 1 EMT). EMT is also associated with wound healing, tissue regeneration and organ fibrosis (type 2 EMT) (12-14). Moreover, EMT occurs in neoplastic cells that have previously undergone genetic and epigenetic changes, specifically in genes that favor clonal outgrowth and the development of localized tumors (type 3 EMT). Upon undergoing EMT, cancer cells acquire migratory and invasiveness properties that allow them to migrate through the ECM, resulting in increased metastatic potential (15,16).

Accumulating evidence suggests a direct link between EMT and acquisition of stem cell characteristics (17). Induction of EMT confers many of the properties of self-renewing stem cells (17,18). These findings suggest that EMT plays an impor-

---

*Correspondence to:* Dr Hiroshi Miyata, Department of Gastroenterological Surgery, Osaka University, Graduate School of Medicine, 2-2 Yamadaoka, Suita, Osaka 565-0871, Japan  
E-mail: hmiyata@gesurg.med.osaka-u.ac.jp

**Key words:** esophageal cancer, chemotherapy resistance, epithelial-mesenchymal transition, snail, E-cadherin

tant role in resistance to chemotherapy, because cancer stem cells are considered responsible for resistance to anticancer treatment, such as chemotherapy and radiotherapy (19-21). A possible association between EMT and chemotherapy resistance is suggested by recent studies on various cancer cells. However, there is virtually no direct clinical evidence that links mesenchymal phenotype to chemoresistance in human malignancies. Moreover, the association between EMT and chemoresistance has not been elucidated in esophageal cancers.

The present study was designed to determine the expression of EMT-related markers, including E-cadherin, snail, ZEB1 and vimentin, in residual tumors after chemotherapy using samples obtained from patients who underwent preoperative chemotherapy for esophageal cancers. The study also investigated the relationship between the expressions of such EMT markers with prognosis of patients who underwent chemotherapy.

## Materials and methods

*Patients and tissue samples.* The 185 tissue samples were obtained from patients who underwent radical esophagectomy with lymph node dissection for thoracic esophageal cancer between 1999 and 2007 at the Department of Gastroenterological Surgery, Graduate School of Medicine, Osaka University (Osaka, Japan). Informed consent was obtained from each patient prior to participation in the study. Of these patients, 93 received preoperative chemotherapy followed by surgery while the remaining 92 patients underwent surgery without preoperative therapy. In 65 of the 93 patients who underwent preoperative chemotherapy followed by surgery, endoscopic biopsy samples were obtained before treatment and used for immunohistochemical analysis. Two courses of 4-week preoperative chemotherapy with cisplatin at 70 mg/m<sup>2</sup>, adriamycin at 35 mg/m<sup>2</sup> by rapid intravenous infusion on Day 1 and 5-FU at 700 mg/m<sup>2</sup> by continuous intravenous infusion on Days 1-7 followed by 3-weeks off were scheduled before surgical treatment (6,22). The median duration of the follow-up period was 46 months (range, 18-78 months). Furthermore, 107 patients (57.8%) died during the follow-up.

*Immunohistochemistry and evaluation.* Resected tumor specimens were fixed with 10% formalin in phosphate-buffered saline (PBS). The paraffin-embedded tissue blocks were sectioned at 4- $\mu$ m slices. The sections were deparaffinized in xylene and dehydrated in graded ethanol. For antigen retrieval, they were incubated in 10 mM citrate buffer at 95°C water bath for 40 min. The endogenous peroxidase activity in the tissue specimens was blocked by incubating the slides in 3% hydrogen peroxide (H<sub>2</sub>O<sub>2</sub>) solution in methanol at room temperature for 20 min. After treatment of the sections with 1% bovine serum albumin for 30 min at room temperature to block nonspecific reactions, all sections were incubated with a primary antibody at working dilution in a humidified chamber at 4°C overnight. The antibodies used in the study were anti-E-cadherin monoclonal antibody (mAb, dilution 1:100, buffer pH 9.0; Dako, Corp., Carpinteria, CA), anti-Snail polyclonal antibody (pAb, dilution 1:100, buffer pH 9.0; Santa Cruz

Biotechnology, Inc., Santa Cruz, CA), anti-vimentin mAb (dilution 1:100, buffer pH 9.0; Santa Cruz Biotechnology, Inc.), anti-ZEB1 mAb (dilution 1:500, buffer pH 6.0; Dako, Corp.), anti- $\beta$ -catenin mAb (dilution 1:100, buffer pH 9.0; Dako, Corp.), anti-N-cadherin pAb (dilution 1:200, buffer pH 9.0; Millipore, Bedford, MA). After incubation with secondary antibodies for 20 min, the reactions were visualized using Vectastain ABC immunoperoxidase kit (Vector Laboratories, Burlington, VT) with 3,3'-diaminobenzidine, which stained the antigen brown, and hematoxylin counterstaining.

Two investigators (J.H. and H.M.) independently evaluated the immunohistochemical sections. The deepest invaded area, called the invasive front, was recorded. The degree of E-cadherin and  $\beta$ -catenin immunostaining was graded as reduced, negative or cytoplasmic immunoreactivity; preserved, strong linear immunoreactivity on the cell membrane (23). The expression levels of nuclear-Snail and cytoplasmic-vimentin, cytoplasmic-ZEB1, membrane- or cytoplasmic-N-cadherin were scored as negative,  $\leq$ 10% positive tumor cells; positive, >10% positive tumor cells (Fig. 1).

*Clinical and histopathological evaluation of response to chemotherapy.* Two weeks after 2 cycles of neoadjuvant chemotherapy, all patients were re-assessed to evaluate the clinical response to chemotherapy by endoscopy, computed tomography (CT) and positron emission tomography (PET). The World Health Organization response criteria for measurable disease and the criteria of the Japanese Society for Esophageal Diseases were used to assess clinical response (24,25). A complete response (CR) was defined as disappearance of all lesions. A CR of the primary tumor represented disappearance of the tumor on CT scan and/or PET scan and endoscopy. A partial response (PR) was defined as >50% reduction in primary tumor size and lymph node metastasis, as confirmed by CT scan. Progressive disease (PD) was defined as >25% increase in the primary tumor or the appearance of new lesions. Stable disease (SD) was defined as neither sufficient decrease to qualify for PR nor sufficient increase to qualify for PD.

Based on the percentage of viable residual tumor cells at the primary site after neoadjuvant chemotherapy, curative effect was classified into five categories. Briefly, the percentage of viable residual tumor cells within the entire cancer tissue was assessed as follows: grade 3, no viable residual tumor cells are evident; grade 2, viable residual tumor cells account for less than one-third of tumor tissue; grade 1b, viable residual tumor cells account for less than one-third or more but less than two-thirds of tumor tissue; grade 1a, viable residual tumor cells account for two-thirds or more tumor tissue; and grade 0, no recognizable histological chemotherapy effect (6,25).

*Statistical analysis.* Statistical analysis of group differences was performed using the  $\chi^2$  test, Fisher's exact test or Mann-Whitney U test. For survival analysis, the Kaplan-Meier method was used to assess survival distribution according to EMT-marker expression and differences in survival were estimated using the log-rank test. The Cox proportional hazards regression model was used to analyze the simultaneous influence of prognostic factors. Wilcoxon signed-ranks test was used to assess the change in E-cadherin and Snail expression

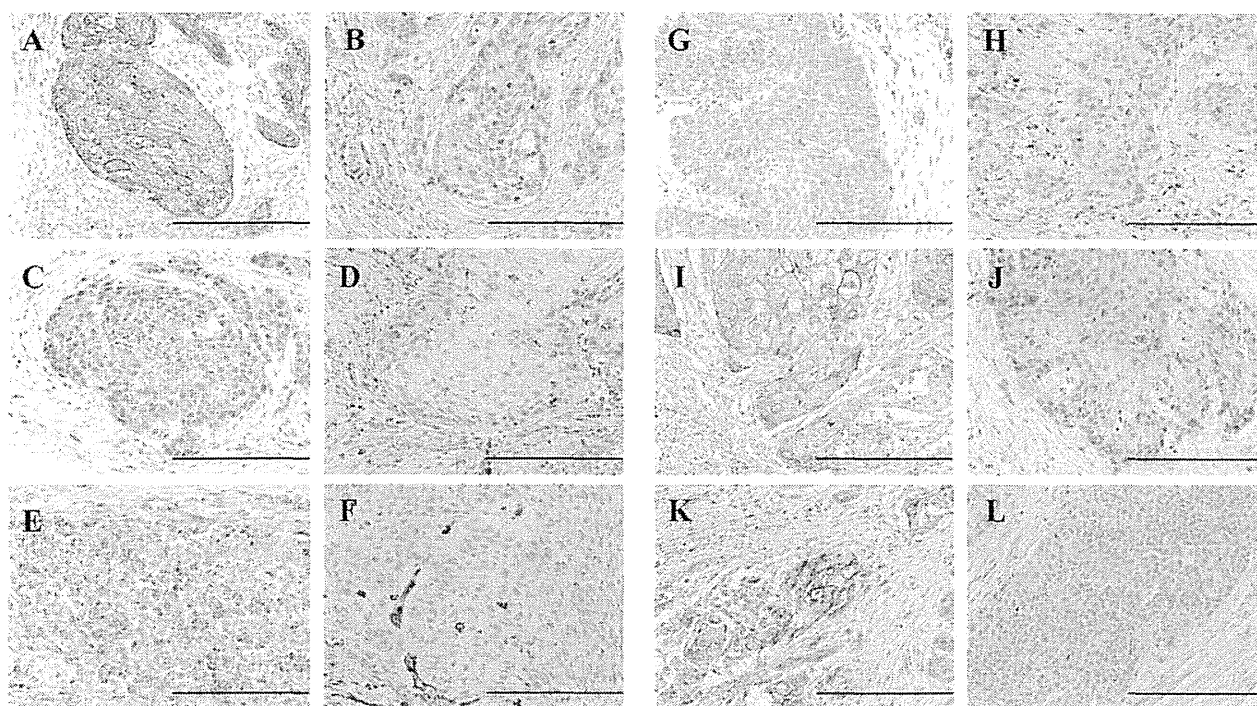


Figure 1. Immunohistochemical expression of E-cadherin, Snail, vimentin, ZEB1,  $\beta$ -catenin and N-cadherin in human esophageal squamous cell carcinoma. We examined the deepest invading area, known as the invasive front. (A) Membranous expression of E-cadherin. (B) Cytoplasmic and negative expression of E-cadherin. (C) Nuclear expression of Snail. (D) Negative nuclear expression of Snail. (E) Cytoplasmic expression of vimentin. (F) Lack of expression of vimentin. (G) Cytoplasmic expression of ZEB1. (H) Negative expression of ZEB1. (I) Membranous expression of  $\beta$ -catenin. (J) Cytoplasmic and negative expression of  $\beta$ -catenin. (K) Membranous or cytoplasmic expression of N-cadherin. (L) Lack of expression of N-cadherin. Magnification, x200.

Table I. Characteristics of 185 patients with esophageal cancer.

	Chemotherapy		P-value
	Residual (n=93)	Naive (n=92)	
Gender (male/female)	79/14	83/9	0.276
Age (mean)	64.0	63.7	0.512
Tumor location (upper/middle/lower)	22/36/35	12/47/33	0.236
Differentiation (G1,2/G3,4)	65/28	75/17	0.418
Depth of invasion (pT1-2/3-4)	32/61	41/51	0.157
Lymph node metastasis (pN0/1)	27/65	33/59	0.345
Lymphatic permeation (positive/negative)	77/16	70/22	0.258
Venous permeation (positive/negative)	52/41	43/49	0.212

after chemotherapy. A P-value of  $<0.05$  denoted the presence of statistically significant difference between groups. All statistical analyses were performed using the software package JMP 8 for Windows (SAS Institute, Inc., Cary, NC).

## Results

*Expression of EMT makers in residual and chemo-naive tumors.* Of the 195 tumors, 93 tumors were residual tumors after preoperative chemotherapy and 92 tumors were chemo-naive tumors without preoperative therapy. There was no significant difference between residual tumors and chemo-naive tumors in differentiation, tumor depth and lymph node metastasis (Table I).

We quantitated the expression of the epithelial marker E-cadherin and mesenchymal markers snail, vimentin, ZEB1, and N-cadherin in residual tumors and chemo-naive tumors (Table II). Fifty percent (46/92) of chemo-naive tumors stained strongly for E-cadherin, while 71% of residual tumors stained weakly for E-cadherin. Statistical analysis indicated significant underexpression of E-cadherin, as a marker of epithelial cells, in residual tumors compared with chemo-naive tumors ( $P=0.003$ ). Snail expression was significantly higher in residual tumors than in chemo-naive tumors ( $P=0.028$ ). Similarly, the expression levels of ZEB1 and N-cadherin were significantly higher in residual tumors than in chemo-naive tumors ( $P<0.001$  and  $P=0.001$ , respectively). However, there were no significant differences in the expression levels of vimentin and  $\beta$ -catenin

Table II. Expression of mesenchymal and epithelial markers in residual tumors after chemotherapy and chemo-naive tumors.

	Chemotherapy			P-value
	Residual (n=93)	Naive (n=92)	Total (n=185)	
E-cadherin				
Preserved	27 (29.0)	46 (50.0)	73 (39.5)	0.003
Reduced	66 (71.0)	46 (50.0)	112 (60.1)	
Snail				
Positive	66 (71.0)	51 (55.4)	117 (63.4)	0.028
Negative	27 (29.0)	41 (44.6)	68 (36.6)	
Vimentin				
Positive	11 (11.8)	8 (8.7)	19 (10.3)	0.482
Negative	82 (88.2)	84 (91.3)	166 (89.7)	
ZEB1				
Positive	36 (38.7)	14 (15.2)	50 (27.0)	<0.001
Negative	57 (61.3)	78 (84.8)	135 (73.0)	
$\beta$ -catenin				
Preserved	32 (34.4)	27 (29.3)	59 (31.9)	0.460
Reduced	61 (65.6)	65 (70.1)	126 (68.1)	
N-cadherin				
Positive	51 (54.8)	29 (31.5)	80 (43.2)	0.001
Negative	42 (45.2)	63 (68.5)	105 (66.8)	

Data are numbers (percentages) of patients.

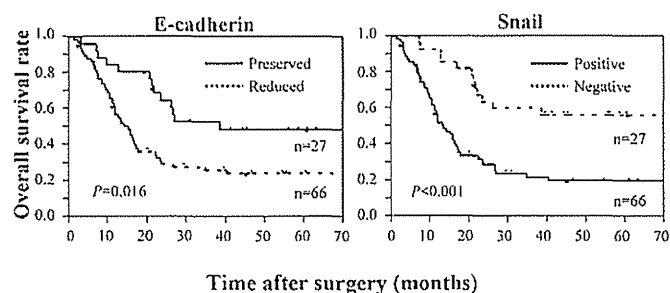


Figure 2. Postoperative overall survival curves according to the immunohistochemical expression of E-cadherin and Snail in the residual group. Left: reduced expression of E-cadherin correlated significantly with short survival of patients of the residual group. Right: high expression of Snail correlated significantly with short survival of patients of the residual group.

between the two types of tumors. Taken together, higher expression of mesenchymal markers and lower expression of epithelial markers characterize residual tumors after chemotherapy.

We examined the relationship between E-cadherin expression, as an epithelial marker, and the expression of several mesenchymal markers (N-cadherin, vimentin, Snail and ZEB1) in the residual group. E-cadherin expression correlated inversely with Snail expression (Table III).

*Relationship between EMT markers and response to chemotherapy.* Next, we examined the relationship between the

Table III. Relationship between expression of E-cadherin and EMT markers in the residual group.

	E-cadherin			P-value
	Preserved (n=27)	Reduced (n=66)	Total (n=93)	
Snail				
Positive	10 (37.0)	56 (84.8)	66 (71.0)	<0.001
Negative	17 (63.0)	10 (15.2)	27 (29.0)	
Vimentin				
Positive	2 (3.7)	9 (13.6)	11 (11.8)	0.379
Negative	25 (96.3)	57 (86.4)	82 (88.1)	
ZEB1				
Positive	8 (29.6)	28 (42.4)	36 (38.7)	0.245
Negative	19 (70.4)	38 (57.6)	57 (61.3)	
$\beta$ -catenin				
Preserved	12 (44.4)	20 (30.3)	32 (34.4)	0.197
Reduced	15 (55.6)	46 (69.7)	61 (65.6)	
N-cadherin				
Positive	17 (63.0)	34 (51.5)	51 (54.8)	0.311
Negative	10 (27.0)	32 (48.5)	42 (45.2)	

Data are numbers (percentages) of patients.

expression of EMT markers and the response to chemotherapy in the residual tumors. With regard to the clinical response, weak E-cadherin expression correlated significantly with clinically poor response (SD/PD), but not with clinically good response (PR) ( $P=0.009$ , Table IV). On the other hand, positive staining for Snail expression in tumors correlated significantly with SD/PD, but not PR ( $P=0.009$ ).

Similar to the clinical response, negative E-cadherin expression and positive staining for Snail expression correlated with histopathologically minor response (Grade 0/1a), but not with major response Grade 1b/2 ( $P=0.001$  and  $P=0.027$ , respectively) (Table V).

*Relationship between EMT markers and survival.* We also examined relationship between the expression of EMT markers and prognosis of patients who underwent preoperative chemotherapy for esophageal cancer. Low expression of E-cadherin correlated significantly with short survival time (Fig. 2). In contrast, high expression of Snail correlated significantly with short survival time (Fig. 2). Multivariate analysis identified Snail expression as an independent prognostic factor, together with tumor depth, in patients who received preoperative chemotherapy for esophageal cancer (Table V).

*Changes in E-cadherin and Snail expression after chemotherapy and survival.* In 65 of 93 patients with esophageal cancer who underwent preoperative chemotherapy followed by surgery, we used immunohistochemistry to compare biopsy samples obtained before chemotherapy with the surgical



Table IV. Relationship between response to chemotherapy and immunohistochemical expression of E-cadherin, Snail, vimentin, ZEB1,  $\beta$ -catenin and N-cadherin in residual tumors.

	Total (n=93)	Clinical response			Pathological response		
		PD/SD (n=47)	PR (n=46)	P-value	Grade 0/1a (n=67)	Grade 1b/2 (n=26)	P-value
<b>E-cadherin</b>							
Preserved	27 (29)	8 (17)	19 (41)	0.009	13 (19)	14 (54)	0.001
Reduced	66 (71)	39 (83)	27 (59)		54 (81)	12 (46)	
<b>Snail</b>							
Positive	66 (71)	39 (83)	27 (59)	0.009	52 (72)	14 (54)	0.027
Negative	27 (29)	8 (17)	19 (41)		15 (22)	12 (46)	
<b>Vimentin</b>							
Positive	11 (12)	5 (11)	6 (13)	0.719	8 (12)	3 (12)	0.957
Negative	82 (88)	42 (89)	40 (87)		59 (88)	23 (88)	
<b>ZEB1</b>							
Positive	36 (39)	15 (31)	21 (46)	0.173	26 (39)	10 (38)	0.976
Negative	57 (61)	32 (68)	25 (54)		41 (61)	16 (62)	
<b><math>\beta</math>-catenin</b>							
Preserved	32 (34)	17 (36)	15 (33)	0.717	23 (34)	9 (35)	0.979
Reduced	61 (66)	30 (64)	31 (67)		44 (66)	17 (65)	
<b>N-cadherin</b>							
Positive	51 (55)	28 (60)	23 (50)	0.353	40 (60)	11 (42)	0.131
Negative	42 (45)	19 (40)	23 (50)		27 (40)	15 (58)	

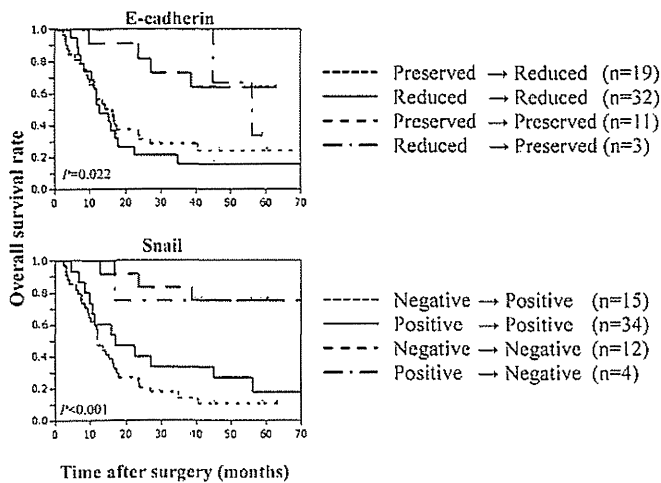


Figure 3. Postoperative overall survival curves according to the immunohistochemical expression of E-cadherin and Snail before and after chemotherapy. Top: short survival of patients (n=51) with decreased expression of E-cadherin after chemotherapy and unchanged low expression of E-cadherin after chemotherapy. Bottom: short survival of patients (n=49) with increased expression of Snail after chemotherapy and unchanged positive expression of Snail after chemotherapy.

specimens after chemotherapy. Among these 65 patients, chemotherapy decreased the expression of E-cadherin in 19 (preserved→reduced) (Table VI). The survival time was significantly shorter in 51 patients with low E-cadherin expression [including the above 19 patients and 32 patients who showed no

change in their low E-cadherin expression after chemotherapy (reduced→reduced)], compared with 11 patients with preserved expression of E-cadherin throughout chemotherapy (Fig. 2). With regard to Snail expression, chemotherapy increased Snail expression in 15 of the 65 patients (negative to positive). The survival time was significantly shorter in 49 patients with positive Snail expression [including the above 15 patients and 34 patients who showed no change in positive Snail expression after chemotherapy (negative to positive)], compared with 12 patients with Snail-negative tumors throughout chemotherapy (Fig. 3).

## Discussion

Although recent evidence indicates that EMT does not only cause increased metastasis but also contributes to chemoresistance, there is no direct clinical evidence for a link between mesenchymal phenotype and chemoresistance in human malignancies. In this study, we examined the expression of EMT-related markers in residual tumors after chemotherapy using samples obtained from patients who underwent preoperative chemotherapy for esophageal cancer. The results showed reduced expression of E-cadherin (a marker of epithelial cells) and increased expression of Snail, ZEB1 and N-cadherin (markers of mesenchymal cells) in residual tumors after chemotherapy, compared with chemo-naïve tumors. Moreover, the reduced expression of E-cadherin and increased expression of snail in residual tumors were significantly asso-

Table V. Univariate and multivariate analyses of prognostic factors.

	Univariate			Multivariate		
	HR	95% CI	P-value	HR	95% CI	P-value
Gender (male/female)	0.84	0.46-1.71	0.619			
Age ( $\leq 65 / > 65$ )	1.22	0.74-2.02	0.422			
Tumor location (upper, middle/lower)	0.73	0.43-1.21	0.225			
Differentiation (G1,2/G3,4)	0.97	0.55-1.74	0.920			
Depth of invasion (pT1-2/pT3-4)	2.49	1.35-5.05	0.003	2.13	1.12-4.37	0.018
Lymph node metastasis (pN0/1)	3.12	2.32-4.21	<0.001	2.12	1.21-4.24	0.009
Lymphatic invasion (positive/negative)	2.09	0.81-3.99	0.181			
Venous invasion (positive/negative)	1.21	0.74-2.02	0.437			
E-cadherin (preserved/reduced)	0.56	0.30-0.98	0.043	1.21	0.63-2.21	0.551
Snail (positive/negative)	3.31	1.78-6.71	<0.001	3.83	1.96-8.11	<0.0001
Vimentin (positive/negative)	0.86	0.38-1.70	0.679			
ZEB1 (positive/negative)	0.88	0.51-1.45	0.617			
$\beta$ -catenin (preserved/reduced)	1.41	0.85-2.33	0.179			
N-cadherin (positive/negative)	0.93	0.56-1.53	0.760			
Clinical response (PD-SD/PR)	2.29	1.38-3.87	0.001	1.68	0.99-2.92	0.052

HR, hazard ratio; 95% CI, 95% confidence interval; PD, progressive disease; SD, stable disease; PR, partial response.

Table VI. Changes in E-cadherin and Snail expression after chemotherapy.

	Pre-CT biopsy	Residual	n	P-value
E-cadherin	Preserved	Reduced	19	<0.001
	Reduced	Reduced	32	
	Preserved	Preserved	11	
	Reduced	Preserved	3	
Snail	Negative	Positive	15	0.019
	Positive	Positive	34	
	Negative	Negative	12	
	Positive	Negative	4	

ciated with poor response to chemotherapy and short survival time in patients who underwent preoperative chemotherapy. These results suggest that residual esophageal tumors after chemotherapy display mesenchymal features, resulting in chemoresistance and poor prognosis.

Reduced expression of E-cadherin, which is a central adhesion molecule located at cell-cell adhesion junctions, is one of the characteristics findings during progression of EMT (26). Previous studies demonstrated that the loss of E-cadherin is associated with tumor progression, tumor metastasis and poor clinical outcome in various human carcinomas (27-31). The association of E-cadherin expression and drug sensitivity has been examined in several types of human cancer. In colorectal cancer, E-cadherin was downregulated in oxaliplatin-resistant colorectal cancer (CRC) cells (28). In gemcitabine-resistance pancreatic cancer cells, E-cadherin expression was decreased and nuclear localization of total  $\beta$ -catenin was increased (30).

While the above studies showed downregulation of E-cadherin in drug-resistant tumor cell lines, there is little or no evidence for the clinical importance of E-cadherin expression in drug-resistant human cancers. Using samples from patients who underwent preoperative chemotherapy for esophageal cancers, we demonstrated in this study the importance of E-cadherin underexpression in chemoresistance in human esophageal cancer.

Snail is recognized as a suppressor of E-cadherin expression. Snail represses the transcription of E-cadherin by binding to the E-box elements in the proximal E-cadherin promoter, thereby triggering a complete EMT and resulting in enhanced tumor invasiveness (30). Accumulating evidence suggests the contribution of Snail expression to therapeutic resistance in various cancers (28-30,33). Paclitaxel-resistant ovarian cancer cells showed upregulation of Snail expression, with marked enhancement of metastatic activity, compared with control cells (30). In head and neck cancer, Snail contributes to cisplatin resistance by upregulating excision repair cross complementation group 1 (ERCC1), which plays a key role in nucleotide excision repair and in platinum-induced DNA adducts (33). In the present study, upregulation of Snail was observed in residual tumors after chemotherapy for esophageal cancers and such high expression was significantly associated with poor response to chemotherapy. These results provide direct evidence for the important role of Snail expression in chemoresistance in human esophageal cancer.

In the present study, we examined the relationship between E-cadherin expression, as an epithelial marker, and the expression of several mesenchymal markers (N-cadherin, vimentin, Snail and ZEB1). In recent years, a switch from E-cadherin to N-cadherin has been often used to monitor the progress of EMT during embryonic development and cancer progression (34). In

our study, although N-cadherin expression was increased in residual tumors, compared with chemo-naïve tumors, we could not find significant inverse relationship between E-cadherin and N-cadherin expression. Snail and ZEB1 are well known transcription repressors of E-cadherin (29,30,32,35), and our results showed inverse correlation between E-cadherin and Snail expression, although we could not find a significant correlation between E-cadherin and ZEB1 expression.

Recent studies have indicated that cancer cells undergoing EMT develop resistance to anticancer drugs. However, it has been difficult to establish the role of EMT in chemoresistance in human clinical samples. In the present study, we investigated whether EMT confers resistance to chemotherapy by comparing the expression of EMT-related markers in residual tumors after chemotherapy with that in chemo-naïve tumors. A few studies have previously shown the presence of EMT in residual tumors after conventional anti-cancer therapy. One such study demonstrated recently mesenchymal features of tumor cells that had survived conventional treatment, such as chemotherapy and endocrine therapy, in human breast cancer (36). The results of the present study demonstrating mesenchymal features of tumor cells after chemotherapy in esophageal cancer provide further support to the above previous studies.

One important problem in the present study is whether tumor cells with initial mesenchymal phenotype survive the chemotherapy or whether residual tumor cells acquire mesenchymal features during chemotherapy. In this study, we compared the expression of EMT-related markers such as E-cadherin and Snail before and after chemotherapy in the same case, and found in certain cases mesenchymal features in residual tumors after chemotherapy compared with epithelial features before treatment. This finding suggests that residual tumor cells seem to acquire mesenchymal features during chemotherapy. However, the value of immunohistochemistry in accurate assessment of gene expression in biopsy samples is limited, because biopsy samples do not allow accurate estimation of such events in the invasive front of tumors. Recent studies have pointed to link between EMT phenotype and development of cancer stem cells; cancer cells undergoing EMT exhibit characteristic markers of cancer stem cells and properties of cancer stem cells (17). However, other studies have suggested that cancer stem cells from solid tumors are not actually static entities but rather tumor cells that transiently acquire stemness properties depending on the tumor context (37), although the traditional concept of cancer stem cells is a unidirectional hierarchical model. These findings suggest that residual esophageal cancer cells may transiently acquire mesenchymal features to survive during chemotherapy. In support of this notion, one recent study showed that cancer cell populations employ a dynamic strategy in which individual cells transiently assume a reversibly drug-tolerant state to protect the remaining population from eradication by exposure to lethal anti-cancer drugs (38). Further studies are required to ascertain whether esophageal cancer cells transiently acquire mesenchymal features and stemness properties during chemotherapy in human esophageal cancers.

In conclusion, the present study demonstrated decreased expression of E-cadherin and increased expression of Snail, ZEB1 and N-cadherin in residual tumors after chemotherapy in human esophageal cancers, compared with chemo-naïve

tumors. Moreover, in patients who underwent preoperative chemotherapy, the reduced expression of E-cadherin and increased expression of Snail in residual tumors correlated significantly with poor response to chemotherapy and poor prognosis. These findings suggest that residual tumors after chemotherapy for esophageal cancer switch to mesenchymal phenotype, resulting in chemoresistance and poor clinical outcome.

### Acknowledgements

This study was supported by a Grant-in-Aid for Young Scientists from the Ministry of Education, Culture, Sports, Science and Technology of Japan.

### References

1. Medical Research Council Oesophageal Cancer Working Group. Surgical resection with or without preoperative chemotherapy in oesophageal cancer: a randomised controlled trial. *Lancet* 359: 1727-1733, 2002.
2. Kelsen DP, Ginsberg R, Pajak TF, Sheahan DG, Gunderson L, Mortimer J, Estes N, Haller DG, Ajani J, Kocha W, *et al*: Chemotherapy followed by surgery compared with surgery alone for localized esophageal cancer. *N Engl J Med* 339: 1979-1984, 1998.
3. Gebski V, Burmeister B, Smithers BM, Foo K, Zalberg J and Simes J: Australasian Gastro-Intestinal Trials Group. Survival benefits from neoadjuvant chemoradiotherapy or chemotherapy in oesophageal carcinoma: a meta-analysis. *Lancet Oncol* 8: 226-234, 2007.
4. Law S, Fok M, Chow S, Chu KM and Wong J: Preoperative chemotherapy versus surgical therapy alone for squamous cell carcinoma of the esophagus: a prospective randomized trial. *J Thorac Cardiovasc Surg* 114: 210-217, 1997.
5. Ando N, Iizuka T, Ide H, Ishida K, Shinoda M, Nishimaki T, Takiyama W, Watanabe H, Isono K, Aoyama N, *et al*: Japan Clinical Oncology Group. Surgery plus chemotherapy compared with surgery alone for localized squamous cell carcinoma of the thoracic esophagus: a Japan Clinical Oncology Group Study - JCOG9204. *J Clin Oncol* 21: 4592-4596, 2003.
6. Yano M, Takachi K, Doki Y, Miyashiro I, Kishi K, Noura S, Eguchi H, Yamada T, Ohue M, Ohgashi H, *et al*: Preoperative chemotherapy for clinically node-positive patients with squamous cell carcinoma of the esophagus. *Dis Esophagus* 19: 158-163, 2006.
7. Tepper J, Krasna MJ, Niedzwiecki D, Hollis D, Reed CE, Goldberg R, Kiel K, Willett C, Sugarbaker D and Mayer R: Phase III trial of trimodality therapy with cisplatin, fluorouracil, radiotherapy, and surgery compared with surgery alone for esophageal cancer: CALGB 9781. *J Clin Oncol* 26: 1086-1092, 2008.
8. Hilgenberg AD, Carey RW, Wilkins EW Jr, Choi NC, Mathisen DJ and Grillo HC: Preoperative chemotherapy, surgical resection, and selective postoperative therapy for squamous cell carcinoma of the esophagus. *Ann Thorac Surg* 45: 357-363, 1998.
9. Ancona E, Ruol A, Santi S, Merigliano S, Sileni VC, Koussis H, Zaninotto G, Bonavina L and Peracchia A: Only pathologic complete response to neoadjuvant chemotherapy improves significantly the long term survival of patients with resectable esophageal squamous cell carcinoma: final report of a randomized, controlled trial of preoperative chemotherapy versus surgery alone. *Cancer* 191: 2165-2174, 2001.
10. Urschel JD, Vasan H and Blewett CJ: A meta-analysis of randomized controlled trials that compared neoadjuvant chemotherapy and surgery to surgery alone for resectable esophageal cancer. *Am J Surg* 183: 274-279, 2002.
11. Kalluri R and Weinberg RA: The basics of epithelial-mesenchymal transition. *J Clin Invest* 119: 1420-1428, 2009.
12. Zeisberg EM, Tarnavski O, Zeisberg M, Dorfman AL, McMullen JR, Gustafsson E, Chandraker A, Yuan X, Pu WT, Roberts AB, *et al*: Endothelial-to-mesenchymal transition contributes to cardiac fibrosis. *Nat Med* 13: 952-961, 2007.
13. Zeisberg M, Yang C, Martino M, Duncan MB, Rieder F, Tanjore H and Kalluri R: Fibroblasts derive from hepatocytes in liver fibrosis via epithelial to mesenchymal transition. *J Biol Chem* 282: 23337-23347, 2007.

14. Kim KK, Kugler MC, Wolters PJ, Robillard L, Galvez MG, Brumwell AN, Sheppard D and Chapman HA: Alveolar epithelial cell mesenchymal transition develops *in vivo* during pulmonary fibrosis and is regulated by the extracellular matrix. *Proc Natl Acad Sci USA* 103: 13180-13185, 2006.
15. Thiery JP: Epithelial-mesenchymal transitions in tumour progression. *Nat Rev Cancer* 2: 442-454, 2002.
16. Yang J and Weinberg RA: Epithelial-mesenchymal transition: at the crossroads of development and tumor metastasis. *Dev Cell* 14: 818-829, 2008.
17. Mani SA, Guo W, Liao MJ, Eaton EN, Ayyanan A, Zhou AY, Brooks M, Reinhard F, Zhang CC, Shipitsin M, *et al*: The epithelial-mesenchymal transition generates cells with properties of stem cells. *Cell* 133: 704-715, 2008.
18. Biddle A, Liang X, Gammon L, Fazil B, Harper LJ, Emich H, Costea DE and Mackenzie IC: Cancer stem cells in squamous cell carcinoma switch between two distinct phenotypes that are preferentially migratory or proliferative. *Cancer Res* 71: 5317-5326, 2011.
19. Kurrey NK, Jalgaonkar SP, Joglekar AV, Ghanate AD, Chaskar PD, Doiphode RY and Bapat SA: Snail and slug mediate radioresistance and chemoresistance by antagonizing p53-mediated apoptosis and acquiring a stem-like phenotype in ovarian cancer cells. *Stem Cells* 27: 2059-2068, 2009.
20. Eyler CE and Rich JN: Survival of the fittest: cancer stem cells in therapeutic resistance and angiogenesis. *J Clin Oncol* 26: 2839-2845, 2008.
21. Baumann M, Krause M and Hill R: Exploring the role of cancer stem cells in radioresistance. *Nat Rev Cancer* 8: 545-554, 2008.
22. Miyata H, Yoshioka A, Yamasaki M, Nushijima Y, Takiguchi S, Fujiwara Y, Nishida T, Mano M, Mori M and Doki Y: Tumor budding in tumor invasive front predicts prognosis and survival of patients with esophageal squamous cell carcinomas receiving neoadjuvant chemotherapy. *Cancer* 115: 3324-3334, 2009.
23. Usami Y, Chiba H, Nakayama F, Ueda J, Matsuda Y, Sawada N, Komori T, Ito A and Yokozaki H: Reduced expression of claudin-7 correlates with invasion and metastasis in squamous cell carcinoma of the esophagus. *Hum Pathol* 37: 569-577, 2006.
24. Miller AB, Hoogstraten B, Staquet M and Winkler A: Reporting results of cancer treatment. *Cancer* 47: 207-214, 1981.
25. Japan Esophageal Society: Japanese classification of esophageal cancer, tenth edition: parts II and III. *Esophagus* 6: 71-94, 2009.
26. Lombaerts M, van Wezel T, Philippo K, Dierssen JW, Zimmermann RM, Oosting J, van Eijk R, Eilers PH, van de Water B, Cornelisse CJ and Cleton-Jansen AM: E-cadherin transcriptional downregulation by promoter methylation but not mutation is related to epithelial-to-mesenchymal transition in breast cancer cell lines. *Br J Cancer* 94: 661-671, 2006.
27. Shiozaki H, Tahara H, Oka H, Miyata M, Kobayashi K, Tamura S, Iihara K, Doki Y, Hirano S, Takeichi M and Mori T: Expression of immunoreactive E-cadherin adhesion molecules in human cancers. *Am J Pathol* 139: 17-23, 1999.
28. Yang AD, Fan F, Camp ER, van Buren G, Liu W, Somcio R, Gray MJ, Cheng H, Hoff PM and Ellis LM: Chronic oxaliplatin resistance induces epithelial-to-mesenchymal transition in colorectal cancer cell lines. *Clin Cancer Res* 12: 4147-4153, 2006.
29. Kajiyama H, Shibata K, Terauchi M, Yamashita M, Ino K, Nawa A and Kikkawa F: Chemoresistance to paclitaxel induces epithelial-mesenchymal transition and enhances metastatic potential for epithelial ovarian carcinoma cells. *Int J Oncol* 31: 277-283, 2007.
30. Shah AN, Summy JM, Zhang J, Park SI, Parikh NU and Gallick GE: Development and characterization of gemcitabine-resistant pancreatic tumor cells. *Ann Surg Oncol* 14: 3629-3637, 2007.
31. Arumugam T, Ramachandran V, Fournier KF, Wang H, Marquis L, Abbruzzese JL, Gallick GE, Logsdon CD, McConkey DJ and Choi W: Epithelial to mesenchymal transition contributes to drug resistance in pancreatic cancer. *Cancer Res* 69: 5820-5828, 2009.
32. Peinado H, Olmeda D and Cano A: Snail, Zeb and bHLH factors in tumour progression: an alliance against the epithelial phenotype? *Nat Rev Cancer* 7: 415-428, 2007.
33. Hsu DS, Lan HY, Huang CH, Tai SK, Chang SY, Tsai TL, Chang CC, Tzeng CH, Wu KJ, Kao JY and Yang MH: Regulation of excision repair cross-complementation group 1 by Snail contributes to cisplatin resistance in head and neck cancer. *Clin Cancer Res* 16: 4561-4571, 2010.
34. Hirohashi S and Kanai Y: Cell adhesion system and human cancer morphogenesis. *Cell Sci* 94: 575-581, 2003.
35. Nieto MA: The snail superfamily of zinc-finger transcription factors. *Nat Rev Mol Cell Biol* 3: 155-166, 2002.
36. Creighton CJ, Li X, Landis M, Dixon JM, Neumeister VM, Sjolund A, Rimm DL, Wong H, Rodriguez A, Herschkowitz JI, *et al*: Residual breast cancers after conventional therapy display mesenchymal as well as tumor-initiating features. *Proc Natl Acad Sci USA* 106: 13820-13825, 2009.
37. Roesch A, Fukunaga-Kalabis M, Schmidt EC, Zabierowski SE, Brafford PA, Vultur A, Basu D, Gimotty P, Vogt T and Herlyn M: A temporarily distinct subpopulation of slow-cycling melanoma cells is required for continuous tumor growth. *Cell* 141: 583-594, 2010.
38. Sharma SV, Lee DY, Li B, Quinlan MP, Takahashi F, Maheswaran S, McDermott U, Azizian N, Zou L, Fischbach MA, *et al*: A chromatin-mediated reversible drug-tolerant state in cancer cell subpopulations. *Cell* 141: 69-80, 2010.

# Magnetic resonance imaging for simultaneous morphological and functional evaluation of esophageal motility disorders

Yasuhiro Miyazaki · Kiyokazu Nakajima · Mitsuhiro Sumikawa · Makoto Yamasaki · Tsuyoshi Takahashi · Hiroshi Miyata · Shuji Takiguchi · Yukinori Kurokawa · Noriyuki Tomiyama · Masaki Mori · Yuichiro Doki

Received: 4 January 2013 / Accepted: 25 February 2013 / Published online: 21 May 2013  
© Springer Japan 2013

## Abstract

**Purposes** The purpose of this study was to evaluate the feasibility and safety of esophageal functional magnetic resonance imaging (fMRI) for the diagnosis of achalasia.

**Methods** Eleven patients with suspected achalasia and three normal subjects underwent fMRI while swallowing clear liquid with original sequences; “T2-weighted single-shot fast spin-echo” and “Fast Imaging Employing Steady-state Acquisition”. The fMRI-based diagnosis was compared with that based on manometry. The luminal fluctuation index (LFI) and Dd/Ds ratio were used for the objective evaluation of the esophageal peristalsis and relaxation of the lower esophageal sphincter (LES).

**Results** Functional MRI showed a dilated tortuous esophagus with no tumor, poor clearance, simultaneous waves, aperistalsis, and impaired LES relaxation in all but one case, allowing the diagnosis of achalasia with accuracy similar to that of manometry. The LFI (median 0.08, range 0.03–0.25) and Dd/Ds ratio (1.40, 1.0–2.3) of the patient group were significantly lower than those of the normal subjects [1.50, 2.32–4.05, and 2.59 (2.32–4.05)]. No severe adverse events directly related to fMRI were noted.

**Conclusions** Using our protocol, fMRI was considered to be safe and feasible for the diagnosis of achalasia. Given the widespread use of MRI, esophageal fMRI, which does not require exposure to radiation, could be a potentially useful diagnostic tool for patients with esophageal motility disorders.

**Keywords** Esophagography · Esophagogastroduodenoscopy · Manometry · Achalasia · Magnetic resonance imaging

## Introduction

Achalasia is an idiopathic primary esophageal motility disorder characterized by esophageal aperistalsis and impaired swallow-induced relaxation of the lower esophageal sphincter (LES). It is a rare disease that affects both genders with a prevalence rate of <1/100,000 per year [1–4]. In addition to the typical symptom of dysphagia for both liquids and solids, patients often present with back pain, chest pain, and/or regurgitation. Although these symptoms provide a hint to the diagnosis of achalasia, it is not unusual for it to take a long time to diagnose this condition due to the lack of specific symptoms or abnormal findings on physical examinations [5, 6]. There have been reports of patients with achalasia and prolonged postprandial reflux who have been treated with an acid secretory inhibitor for long periods under the misdiagnosis of gastroesophageal reflux disease (GERD) [7]. Care must be taken to avoid a misdiagnosis of various diseases mimicking achalasia, including cases with esophageal cancer, known as “pseudoachalasia”.

The investigative work-up for dysphagia includes esophagography, esophagogastroduodenoscopy (EGD), and chest/abdominal computed tomography (CT). These modalities are often repeated before sending patients to a

Y. Miyazaki · K. Nakajima (✉) · M. Yamasaki · T. Takahashi · H. Miyata · S. Takiguchi · Y. Kurokawa · M. Mori · Y. Doki

Division of Gastroenterological Surgery, Department of Surgery, Graduate School of Medicine, Osaka University, 2-2 E-2 Yamadaoka, Suita, Osaka 565-0871, Japan  
e-mail: knakajima@gesurg.med.osaka-u.ac.jp

Y. Miyazaki  
e-mail: ymiyazaki02@gesurg.med.osaka-u.ac.jp

M. Sumikawa · N. Tomiyama  
Department of Radiology, Graduate School of Medicine, Osaka University, 2-2 E-2 Yamadaoka, Suita, Osaka 565-0871, Japan

physiological laboratory for esophageal manometry, resulting in a long morbidity period prior to active treatment. A single diagnostic procedure that can evaluate the esophageal morphology and function in one setting may provide an earlier diagnosis, thus benefiting patients by avoiding a prolonged inflammation period. Reducing the pretreatment period may lead to more successful surgery with fewer complications, lower healthcare expenses, and thus, a better overall improvement of the outcome.

Functional magnetic resonance imaging (fMRI) has been widely applied for the diagnosis of a variety of diseases following advances in the development of fast imaging techniques and improved resolution. Although fMRI is currently used in the clinical setting for the evaluation of cardiac and/or macrovascular diseases [8], several reports have advocated using MRI for the functional testing of the esophagus [9–11]. However, the imaging methods described in the literature have varied widely and are all used different types of contrast media. Presently, fMRI is not established as a diagnostic modality for esophageal motility disorders. In addition, there are no objective criteria for the diagnosis of achalasia with fMRI.

We hypothesized that optimization of the imaging sequences would enhance the use of esophageal fMRI without contrast medium, as an investigative modality for achalasia. To test this hypothesis, we evaluated the feasibility, safety, and potential effectiveness of esophageal fMRI with optimized imaging sequences. Based on the findings of the study, we propose new numerical indices for the objective evaluation of esophageal motility using fMRI.

## Materials and methods

### Patients

From April 2010 to October 2011, 11 consecutive patients (four males, seven females, median age 40, range 27–77 years) were referred to our hospital with esophageal obstructive symptoms, e.g., progressive dysphagia, reflux of undigested food and retrosternal chest pain. All patients underwent an initial workup using esophagography, EGD and chest/abdominal CT. In addition, these patients underwent esophageal fMRI according to the imaging protocols described below. A definite diagnosis was made by esophageal manometry. Patients with a confirmed diagnosis of achalasia underwent a laparoscopic Heller-Dor operation. The remaining patients received appropriate treatment depending on the final diagnosis.

### Imaging protocols

All patients fasted overnight to empty the esophagus and reduce the risk of aspiration. Two imaging protocols were

used on a 3.0 T MRI unit (Signa, General Electric, Milwaukee, WI):

### *SSFSE to fixed-slice angles*

Axial T2-weighted single-shot fast spin-echo (SSFSE) MR imaging (TR 1000 ms, TE 80 ms, Bandwidth 62.5, Frequency 288, Phase 160, FOV 35.0 cm, Slice thickness 8 mm, Spacing 1 mm, Asset sense factor 2) was performed from the level of the sternal notch to the upper abdomen, to determine the optimum slice angles for the esophageal body where the longest sagittal slice was required, and the LES, where esophageal motility could be evaluated in a reproducible fashion. In patients with a severely tortuous esophagus, more than two slice angles at one location and oblique images at the esophageal body were necessary to provide an adequate evaluation of the motility.

### *FIESTA for fMRI*

First, one series of dynamic acquisitions for 40 s, consisting of SSFSE sequences at the esophageal body, was obtained during 30-s water swallowing, followed by rest for 10 s at the confirmed slice angle. Esophageal fMRI was then performed using a Fast Imaging Employing Steady-state Acquisition (FIESTA) sequence, under the following settings: TR 3.5 ms, TE 1.5 ms, Flip angle 40°, Bandwidth 125, Frequency 256, Phase 256, FOV 35.0 cm, Slice thickness 8 mm, and Asset sense factor 1.5. Additional images were obtained using the same protocol at the level of the LES.

### Image interpretation

The morphological evaluation included the presence and extent of esophageal dilation (maximal diameter), tortuous changes, and the presence or absence of tumorous lesions. The esophageal motility was expressed by the following parameters: esophageal peristalsis, swallow-induced LES relaxation, presence of simultaneous waves and the esophageal clearance. The obtained images were interpreted by one independent radiologist who was blinded to the results of the other imaging studies and physiological tests.

### *Morphology*

1. *Esophageal dilation* the maximal diameter of the esophagus was measured on the axial SSFSE images, and esophageal dilation was defined as an esophageal diameter >3.5 cm.
2. *Tortuous esophagus* the center of the esophagus was plotted at each level with axial SSFSE images.

Esophageal meandering was defined on the basis of shifted plots over the esophageal radius.

3. *Tumorous lesions* neoplasms responsible for dysphagia or esophageal dilatation, including esophageal and extra-esophageal lesions.

#### Motility

1. *Simultaneous waves* defined when both the anterior and posterior walls of the esophagus seemed to twitch several times at the pleural sites on FIESTA images of the esophageal body.
2. *Esophageal clearance* FIESTA images of the esophageal body were obtained with a clear liquid swallow. When the entire liquid volume entered the stomach, the esophageal clearance was labeled as “good” clearance; otherwise, it was defined as “poor” clearance.
3. *Peristalsis* both SSFSE and FIESTA images of the esophageal body were obtained under continuous liquid swallow. When the esophagus showed contractions and relaxations in response to swallowing, and the intra-esophageal liquid moved into the stomach at the same time, peristalsis was regarded as “positive”; otherwise it was considered to be “negative”.
4. *Impaired LES relaxation* this was diagnosed by the absence of timely/complete distension of the esophageal lumen above the esophagogastric junction following swallowing.

#### Numerical indices

Three healthy male subjects (median age 34, range 33–35 years) underwent fMRI using the above protocols. The following two indices were applied for a more objective and precise evaluation of the esophageal peristalsis and LES relaxation.

#### LFI for peristalsis

The diameter of the esophageal body was continuously measured for 20 s using SSFSE at the level of two-vertebra-length region from cranium to the diaphragm. The minimal diameter was first determined by reviewing 20 of the obtained sequences. Each diameter at every second was then divided by the minimal diameter and was expressed as the “diameter ratio.” The maximal diameter ratio (Rmax) and standard deviation value of all 20 ratios (SDratio) were calculated. The luminal fluctuation index (LFI) was defined by the following formula:  $LFI = R_{max} \times SD_{ratio}$ . The larger the degree and the higher the frequency of contraction and relaxation motility of the esophagus were, the

higher the LFI score was. The presence/absence of esophageal peristalsis was determined by comparing the LFI between patients and normal subjects.

#### Dd/Ds for LES relaxation

The changes in the esophageal diameter were measured at the level of the LES using both SSFSE and FIESTA sequences. The “Dd” and “Ds” were defined as the maximal and minimal diameters during the liquid swallow, respectively.

#### Safety of fMRI

Any adverse events related to fMRI and the time required to complete the fMRI study were recorded. All adverse events were evaluated based on the Common Terminology Criteria for Adverse Events (CTCAE) version 4.

#### Statistical analysis

Data were expressed as the median (range) values. The Wilcoxon paired signed rank test was used to compare the LFI and Dd/Ds between patients and healthy volunteers. The analysis was carried out with the JMP version 8.0 software program (SAS Institute Inc., Cary, NC), and a two-sided  $p$  value  $<0.05$  was considered to be significant.

#### Results

Table 1 shows the demographics of the 11 patients with suspected achalasia and the initial work-up findings based on esophagography, EGD and chest/abdominal CT. The time from onset to final diagnosis ranged from two to 24 years (median seven years). Seven patients had received treatment for dysphagia before enrollment in the present study with pneumatic balloon dilatation and/or the administration of a calcium channel blocker. The initial work-up showed a dilated-tortuous esophagus in 10 of the 11 patients. No tumorous lesion was detected in any of the patients. Simultaneous waves were detected in three patients by esophagography only. The assessment of the esophageal clearance by esophagography was different from that by EGD. Since all patients had excess residue in the esophagus observed on EGD, they were considered to have poor clearance. Peristalsis and impaired LES relaxation could not be assessed by the initial work-up.

The established diagnosis using manometry was achalasia in 10 patients and a hypertensive LES in one patient. A Laparoscopic Heller-Dor operation was performed in all 10 achalasia patients without any intraoperative complications. The median length of the operation was 191

**Table 1** Patients' demographics and the initial work-up findings using esophagography, EGD and chest/abdominal CT ( $n = 11$ )

Parameters		Number of patients		
Gender, male/female		4/7 <sup>a</sup>		
Age, years		40.0 (27–77)		
Body mass index, kg/m <sup>2</sup>		18.9 (16.5–22.1)		
Duration of symptoms, years		7.0 (2–24)		
Prior treatment				
Yes/no		7/4		
Balloon dilatation		4		
Calcium channel blocker		3		
		Esophagography	EGD	Chest/abdominal CT
Maximal diameter, cm		4.5 (1.8–6.2)		
Dilation		Yes/no	10/1	10/1
Tortuous changes		Yes/no	10/1	10/1
Tumorous lesion		Yes/no	0/11	0/11
Simultaneous waves		Yes/no	3/8	
Esophageal clearance		Good/poor	5/6	0/11

Data are the number of patients, or the median and range

EGD esophagogastroduodenoscopy

(150–292) minutes, with minimal blood loss. All patients showed rapid postoperative recovery, with complete resolution of their preoperative clinical symptoms. The other remaining patient with a hypertensive LES received medical treatment with amlodipine besilate (10 mg/day), which resulted in partial relief of the dysphagia.

#### Feasibility of fMRI

Table 2 compares the results of the evaluation of each parameter and the diagnosis obtained with fMRI and manometry.

**Table 2** Comparison between functional MRI and manometry

		Functional MRI	Manometry
Maximal diameter, cm		4.5 (1.9–5.4)	
Dilation		Yes/no	9/2
Tortuous changes		Yes/no	10/1
Tumorous lesion		Yes/no	0/11
Simultaneous waves		Yes/no	9/2
Esophageal clearance		Good/poor	1/10
Peristalsis		Yes/no	0/11
LES relaxation		Yes/no	0/7
Diagnosis			
Achalasia		10	10
Other disease		1 <sup>a</sup>	1 <sup>a</sup>

LES lower esophageal sphincter

<sup>a</sup> This case corresponded to the patient (Case 5) who was finally diagnosed to have a hypertensive LES

#### Morphology

1. *Esophageal dilation* the maximal diameter of the esophagus ranged from 1.9 to 5.4 cm (median 4.5 cm). Nine patients were considered to have esophageal dilation, whereas the maximal diameter was 1.9 cm and 2.9 cm in the other two cases (Case 5 and Case 8, respectively).
2. *Tortuous esophagus* this morphology was observed in all but one patient (Case 5).
3. *Tumorous lesions* no tumor was detected in any of the patients.

#### Motility

1. *Simultaneous waves*: Figure 1 shows the typical findings of simultaneous waves. They were detected in all but two patients (Case 5 and Case 11).
2. *Esophageal clearance*: Poor esophageal clearance was noted in 10 patients. The swallowed liquid remained in the esophagus in all but one patient (Case 5).
3. *Peristalsis*: All patients exhibited aperistalsis.
4. *Impaired relaxation of the LES*: although this could not be assessed in four patients due to severe tortuosity and adverse events such as nausea and vomiting during the MRI scans, impaired relaxation of the LES was evident in the remaining seven patients.

Based on the fMRI findings described above, all but one patient (Case 5) were diagnosed with achalasia. Since Case 5 had normal esophageal morphology and normal clearance, achalasia was ruled out. The manometric findings confirmed that all 10 patients diagnosed with achalasia by fMRI had



the condition. Case 5 was diagnosed with a hypertensive LES based on manometric findings of rhythmic waves, LES relaxation, and a high LES resting pressure.



**Fig. 1** Simultaneous pressure waves were often observed with the FIESTA sequence

#### LFI and Dd/Ds ratio

In the healthy volunteer group, fMRI visualized the movement of the swallowed liquid and contraction-relaxation motility which induced esophageal emptying (Fig. 2). In these subjects, no residual water was detected in the esophagus during fMRI.

#### Changes in the diameter ratio and LFI

Figure 3 shows the changes in the “diameter ratio” and LFI value in healthy volunteers and patients. The plotted data clearly show that there were marked changes in the esophageal diameter at rest in healthy volunteers compared with the patients with achalasia. The median LFI of the healthy group was 1.50 (range 1.13–1.73), which was significantly higher than that of the patients (median 0.08, range 0.03–0.25,  $p < 0.05$ ). Thus, the diameter ratio allowed the diagnosis of aperistalsis in all 11 patients.

#### Dd/Ds ratio

This ratio was measured on the sagittal fMRI of the normal subjects. In one normal subject, the ratio was also measured on the axial images. In the three normal subjects in

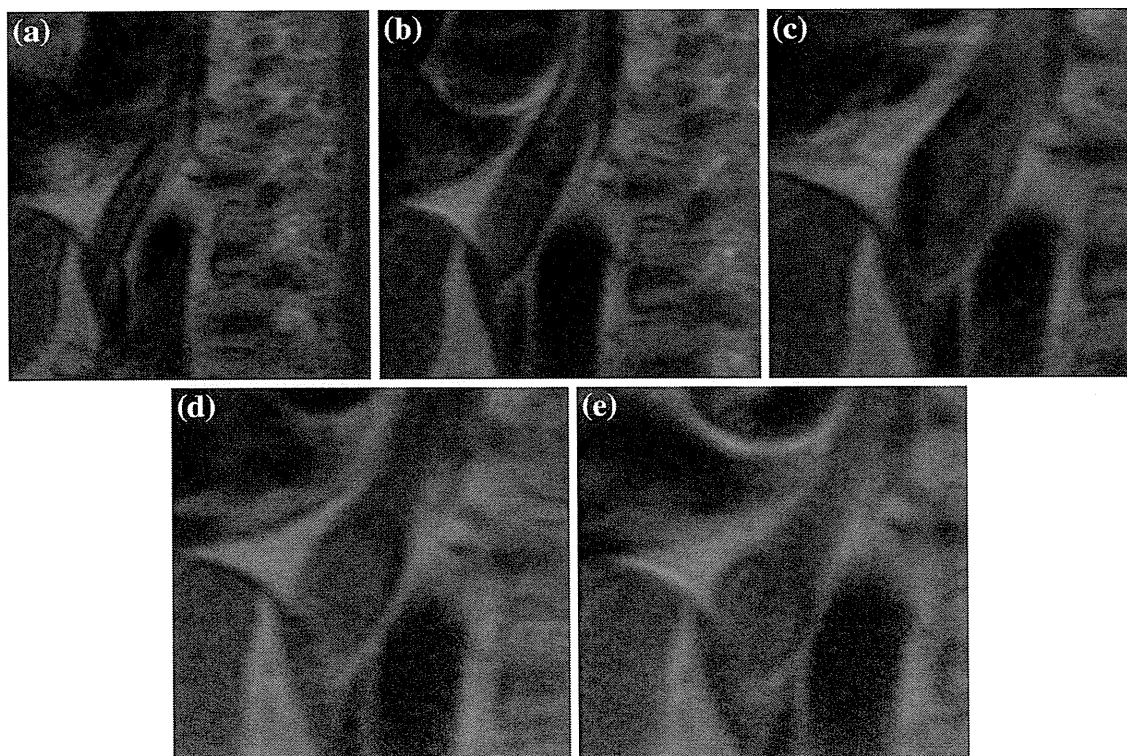


**Fig. 2** Functional MRI allowed the visualization of the movement of the swallowed liquid and esophageal contraction-relaxation motility, which induced esophageal emptying in the normal subjects group

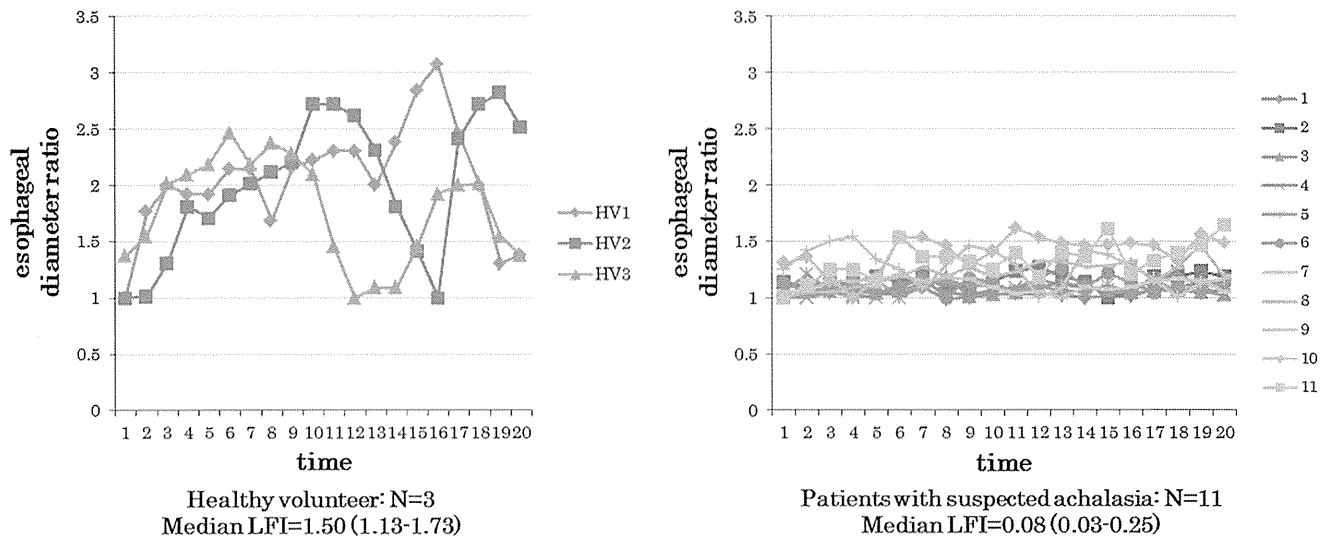


**Fig. 3** The changes in the esophageal diameter ratio and LFI score. *Left* normal subjects, showing esophageal peristalsis, *right* patients with achalasia showed no obvious change in the diameter. The LFI

score of healthy volunteers was significantly higher than that of the patients (Wilcoxon paired signed rank test,  $p < 0.05$ )

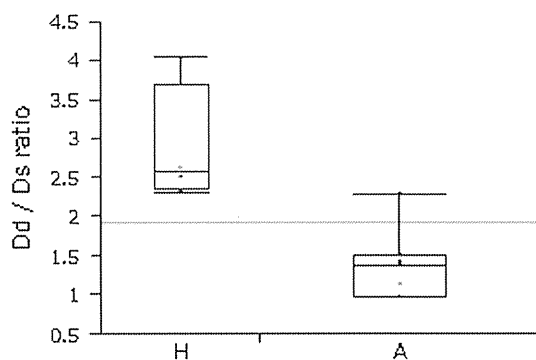


**Fig. 4** Box-and-whisker plots of the Dd/Ds ratios in normal healthy subjects (H) and patients with achalasia (A). In these plots, the lines within the boxes represent median values; the upper and lower lines of the boxes represent the 25th and 75th percentiles, respectively, and the upper and lower bars outside the boxes represent the 90th and 10th percentiles, respectively. ( $p < 0.05$ , by Wilcoxon paired signed rank test)

whom this variable was measured, the median Dd/Ds ratio was 2.59 (range 2.32–4.05). In the patient group, the images of the sagittal slices were not available from four patients due to the tortuous esophagus. Thus, the Dd/Ds ratio was calculated based on the axial images in seven patients. Since the esophageal lumen remained closed throughout water swallowing in one patient (Case 8) and the estimated diameter was 0.0 cm, the Dd/Ds ratio of this patient was considered to be 1.00. The median Dd/Ds ratio of the seven patients (1.40, range 1.00–2.30) was significantly lower than that of the control subjects ( $p < 0.05$ , Fig. 4). These measurements indicated the lack of LES relaxation in all seven patients.

#### Safety of fMRI

No severe side effects (corresponding to more than grade 3 in the CTCAE criteria) were observed in any of the subjects. While no adverse events were recorded in the healthy subjects, several grade 1 events were reported by patients with achalasia, including chest pain, nausea, and vomiting. The time taken to complete the fMRI study was about 30 min.

#### Discussion

The main symptoms of achalasia are dysphasia, chest pain, and backache (so called “achalasia pain”). Although such symptoms are suggestive of achalasia, the diagnosis is often not established for two to three years from the appearance of symptoms [5]. EGD is often the first test used to evaluate dysphasia of esophageal origin and can show esophageal dilation, retention of food or fluid, and a closed LES with a puckered appearance after air insufflation. However, patients with early-stage achalasia are unlikely to show any of the above symptoms, and resistance at the esophagogastric junction may be misinterpreted as peptic stricture, especially when the preliminary diagnosis is GERD [12]. Eckardt et al. [6] stated that the early diagnosis of achalasia could be enhanced if all patients with dysphasia and normal endoscopic findings had their X-rays re-viewed by a second observer and if manometry was performed in cases with equivocal or negative results. On the other hand, additional tests are rarely recommended for patients with normal findings at the first examination.

The use of fMRI to improve the temporal and spatial resolution has recently been proposed for the digestive system, especially for the abdominal cavity. Ajaj et al. [13] reported that gastric peristalsis could be assessed by fMRI using the “gastric motility index”. They compared this index in normal subjects and patients with gastric paresis. More recently, several groups used fMRI to evaluate esophageal peristalsis, LES relaxation and clearance [10]. However, several problems currently hinder the use of fMRI for the assessment of esophageal motility, mainly due to the unique anatomy and physiology of the esophagus. These include its very thin wall, frequent presence of collapsed walls, low-wave amplitudes and higher peristaltic velocity compared with the stomach [13, 14]. To resolve these problems, special contrast media, such as gadolinium-based agents or a ferric ammonium citrate-based solution, were used in previous studies [9–11]. Unfortunately, these types of media cannot be used in patients with dysphagia due to the risk of aspiration.

The present study is the first to describe the potential usefulness of esophageal fMRI with a clear liquid swallow for the diagnosis of achalasia, using several parameters specific to achalasia, and reporting novel indices for diagnosing achalasia. Since any diagnostic modality must be safe and convenient, it is preferable to adopt clear liquid and easy-to-use image sequences. These two points encouraged us to utilize two types of fMRI sequences, SSFSE and FIESTA, which employ T2-weighted images, and which are frequently used in the thoracic field. Since SSFSE has two merits (i.e., small artifacts and good temporal resolution), this sequence is suitable for imaging esophageal wall movements. Furthermore, the FIESTA sequence, which is commonly used in the field of cardiac and macrovascular diseases, shows a higher intensity level of clear liquid in the esophagus. Accordingly, it allows for clearer images of the swallowed water and changes in the esophageal wall elicited by the passage of water to be observed. Thus, the FIESTA images resemble barium esophagography and are appropriate for examining the esophageal lumen morphology and esophageal clearance.

In this study, several parameters specific to achalasia and numerical indices for an objective evaluation were adopted. They allowed for a comparison of the diagnostic ability of different parameters. Table 2 shows the results of the evaluation of each parameter and its usefulness for the diagnosis, with a comparison to the results of manometry. The morphological assessment by fMRI was comparable to that of the initial work-up when using the following parameters: dilation, tortuosity, and the presence or absence of an esophageal tumor. The motility was examined using four parameters. The sensitivity in the diagnosis using simultaneous waves was superior to that of esophagography and was similar to that of manometry, probably

due to the longer observation time and retention of a larger amount of the contrast medium in the esophagus. With regard to the evaluation of esophageal clearance, fMRI obtained with the subject in the supine position more clearly demonstrated poor esophageal clearance in patients with achalasia, compared with esophagography in the standing position. This probably explains the larger number of patients diagnosed with poor clearance by fMRI (10 cases) compared with esophagography (six cases). The results of the assessment of peristalsis and impaired relaxation of the LES by fMRI were similar to those by manometry, with the exception of one patient (Case 5), and the reason(s) for the discrepancy in this case remains unknown. In addition to its diagnostic ability, fMRI is both safe and free of serious side effects. Although more than half of the patients with achalasia reported nausea and one patient suffered vomiting, none developed aspiration pneumonia.

Although a few previous reports assessed the esophageal peristalsis and LES relaxation by fMRI [9–11, 15], these evaluations were subjective and qualitative. In the present study, however, we used two novel objective indices; the LFI and Dd/Ds ratio. The use of cutoff values for the LFI and Dd/Ds ratio allowed us to diagnose aperistalsis and impaired LES relaxation in patients with achalasia. Therefore, the use of the “diameter ratio” and the above indices allows for the objective and semi-quantitative assessment of esophageal motility.

Table 3 provides the results of the comparative analysis of the diagnostic ability of each modality. The conventional modalities, such as esophagography, EGD and chest/abdominal CT, are mainly used for morphological assessment, not the functional analysis. Although esophagography is beneficial for evaluating the esophageal clearance using the “timed-barium esophagography” technique [16], it did not provide an adequate assessment of the esophageal peristalsis and LES relaxation. Patients with dysphagia are initially examined by these modalities, which can rule out the presence of tumorous lesions. However, negative findings with typical morphological features are not uncommon in early-stage achalasia. In addition, repeated esophagography/CTs are associated with a higher risk of radiation exposure. In contrast, fMRI can provide simultaneous morphological and functional evaluation without any risk of radiation. fMRI is thus considered to be potentially useful in the assessment of patients with dysphagia.

Further studies are needed to refine our sequences and imaging protocols to allow for the differentiation of achalasia from other esophageal functional diseases, such as hypertensive LES, diffuse esophageal spasm, nutcracker esophagus, and nonspecific esophageal motility disorders. At present, the differential diagnosis of esophageal functional motility disorders requires manometric recording. It

**Table 3** Diagnostic ability of various modalities according to the morphological and motility parameters

Modality	Morphology			Motility			
	Dilation	Tortuous Change	Tumorous lesion	Simultaneous waves	Esophageal clearance	Peristalsis	Impaired LES relaxation
Esophagography	[Gray crossbar]			[Gray crossbar]			
EGD	[Gray crossbar]			[Gray crossbar]			
chest/abdominal CT	[Gray crossbar]			[Gray crossbar]			
fMRI	[Gray crossbar]			[Gray crossbar]			

Gray crossbars express the spectrum of diagnostic capacity for each parameter  
*LES* Lower esophageal sphincter, *fMRI* functional magnetic resonance imaging

should be kept in mind that confirmation of achalasia is currently not possible using fMRI alone.

From the standpoint of the medical expense, MRI is currently two to three times more expensive than esophagography, EGD, and manometry when the costs are calculated based on the national health insurance price listing in Japan. However, its cost will be gradually decreased with its widespread use in daily clinical practice. When its cost and temporal/spatial resolution become comparable to those of the current CT studies, MRI can represent an attractive screening modality that can be used for the assessment of esophageal motility disorders.

In conclusion, our protocol successfully demonstrated fMRI to be a feasible and safe method for the diagnosis of achalasia. The results of this study suggest that fMRI may be a useful screening tool for esophageal motility disorders.

**Acknowledgments** The authors thank Hisayoshi Kawahara from the Department of Pediatric Surgery, Osaka Medical Center and Research Institute for Maternal and Child Health, for providing expert advice about esophageal motility disorders.

**Conflict of interest** No author has any conflict of interest to declare with regard to this manuscript.

## References

- Spechler SJ, Castell DO. Classification of oesophageal motility abnormalities. *Gut*. 2001;49:145–51.
- Park W, Vaezi MF. Etiology and pathogenesis of achalasia: the current understanding. *Am J Gastroenterol*. 2005;100:1404–14.
- Birgisson S, Richter JE. Achalasia: what's new in diagnosis and treatment? *Dig Dis*. 1997;15(Suppl 1):1–27.
- Mayberry J. F. Epidemiology and demographics of achalasia. *Gastrointest Endosc Clin N Am*. 2001;11:235–248, v.
- Pohl D, Tutuian R. Achalasia: an overview of diagnosis and treatment. *J Gastrointest Liver Dis*. 2007;16:297–303.
- Eckardt VF, Kohne U, Junginger T, Westemeier T. Risk factors for diagnostic delay in achalasia. *Dig Dis Sci*. 1997;42:580–5.
- Kessing BF, Bredenoord AJ, Smout AJ. Erroneous diagnosis of gastroesophageal reflux disease in achalasia. *Clin Gastroenterol Hepatol*. 2011;9:1020–4.
- Poustchi-Amin M, Gutierrez FR, Brown JJ, Mirowitz SA, Narra VR, Takahashi N, et al. Performing cardiac MR imaging: an overview. *Magn Reson Imaging Clin N Am*. 2003;11:1–18.
- Manabe T, Kawamitsu H, Higashino T, Lee H, Fujii M, Hoshi H, et al. Esophageal magnetic resonance fluoroscopy: optimization of the sequence. *J Comput Assist Tomogr*. 2004;28:697–703.
- Panebianco V, Habib FI, Tomei E, Paolantonio P, Anzidei M, Laghi A, et al. Initial experience with magnetic resonance fluoroscopy in the evaluation of oesophageal motility disorders. Comparison with manometry and barium fluoroscopy. *Eur Radiol*. 2006;16:1926–33.
- Covotta F, Piretta L, Badiali D, Laghi A, Biondi T, Corazzari ES, et al. Functional magnetic resonance in the evaluation of oesophageal motility disorders. *Gastroenterol Res Pract*. 2011;2011:367639.
- Richter JE. The diagnosis and misdiagnosis of Achalasia: it does not have to be so difficult. *Clin Gastroenterol Hepatol*. 2011;9:1010–1.
- Ajaj W, Goehde SC, Papanikolaou N, Holtmann G, Ruehm SG, Debatin JF, et al. Real time high resolution magnetic resonance imaging for the assessment of gastric motility disorders. *Gut*. 2004;53:1256–61.
- Richter JE, Wu WC, Johns DN, Blackwell JN, Nelson JL 3rd, Castell JA, et al. Esophageal manometry in 95 healthy adult volunteers. Variability of pressures with age and frequency of “abnormal” contractions. *Dig Dis Sci*. 1987;32:583–92.